Cell, Vol. 89, 287–296, April 18, 1997, Copyright ©1997 by Cell Press

Targeted Gene Disruption Shows That Knobs Enable Malaria-Infected Red Cells to Cytoadhere under Physiological Shear Stress

Brendan S. Crabb,* Brian M. Cooke,† John C. Reeder,* Ross F. Waller,‡ Sonia R. Caruana,* Kathleen M. Davern,* Mark E. Wickham,* Graham V. Brown,* Ross L. Coppel,† and Alan F. Cowman*

*The Walter and Eliza Hall Institute of Medical Research
Melbourne 3050
Australia

†Department of Microbiology
Monash University
Clayton 3168
Australia

‡Plant Cell Biology Research Center
Department of Botany
University of Melbourne
Parkville 3052
Australia

Summary

Knobs at the surface of erythrocytes infected with Plasmodium falciparum have been proposed to be important in adherence of these cells to the vascular endothelium. This structure contains the knob-associated histidine-rich protein (KAHRP) and the adhesion receptor P. falciparum erythrocyte membrane protein 1. We have disrupted the gene encoding KAHRP and show that it is essential for knob formation. Knob$^-$ transfectants adhere to CD36 in static assays; when tested under flow conditions that mimic those of postcapillary venules, however, the binding to CD36 was dramatically reduced. These data suggest that knobs on P. falciparum-infected erythrocytes exert an important influence on adherence of parasitized-erythrocytes to microvascular endothelium, an important process in the pathogenesis of P. falciparum infections.

Introduction

The etiological agent responsible for the most severe form of human malaria is the intraerythrocytic protozoan parasite Plasmodium falciparum. Clinical manifestations of P. falciparum malaria include cerebral malaria, which is the major cause of death from this disease, whereby infected erythrocytes sequester in the deep vascular beds of the brain (MacPherson et al., 1985; Aikawa, 1988). During growth of the asexual stage of the parasite in human erythrocytes, a series of dramatic and extensive changes occur in the structural and functional properties of the infected erythrocyte, which includes development of the ability to adhere to endothelium (Udeinya et al., 1981). Crucial to these changes are proteins of parasite origin that are either deposited on the inner aspect of the erythrocyte membrane or inserted into it (Kilejian and Jensen, 1977; Howard et al., 1988). Recent studies have concentrated on elucidating the interactions of these proteins with various ligands on endothelial cells and uninfected erythrocytes, and their role in the pathogenesis of cerebral malaria (Barnwell et al., 1989; Berendt et al., 1989; Ockenhouse et al., 1992; Wahlgren et al., 1994; Rogerson et al., 1995).

Morphological changes in infected red cells include the appearance of thousands of small protrusions at the cell surface termed knobs (Kilejian, 1979). These consist of an electron-dense cup-shaped structure that underlies a protrusion of the erythrocyte membrane that follows the contour of the cup. Several parasite proteins are present at the cytoplasmic side of the knob structure, including the 85–110 kDa knob-associated histidine-rich protein (KAHRP) (Culvenor et al., 1987; Pologe et al., 1987). The adhesive changes in infected cells are due to the expression of the 200–350 kDa antigenically variant P. falciparum erythrocyte membrane protein 1 (PfEMP1), which appears to be concentrated on the exterior surface of knobs (Baruch et al., 1995). PfEMP1 is encoded by a multi-gene family (Baruch et al., 1995; Su et al., 1995), and expression of variant forms of PfEMP1 enables antigenic variation and expression of a receptor with differing ligand-binding properties (Smith et al., 1995). The functional role of knobs has been controversial. Some studies have suggested that knobs are essential for cytoadherence (Langreth and Peterson, 1985; Raventos et al., 1985), while others have demonstrated that they are not required for cytoadherence to melanoma cells or purified CD36 (Biggs et al., 1989, 1990; Udomsangpetch et al., 1989).

Much of our understanding of the function of parasite proteins at the membrane skeleton has come from the study of P. falciparum lines propagated in in vitro culture that have undergone spontaneous chromosome breakages, which result in the loss of structural genes (Corcoran et al., 1986; Pologe and Ravetch, 1986). For example, lines that have lost approximately 200 kb from one end of chromosome 2, a region that includes the *KAHRP* gene, do not express knob structures (Pologe and Ravetch, 1986). Ascribing the knob structure to expression of the gene encoding KAHRP is problematic, as many other genes are lost in this deletion event including *PfEMP3* (Lanzer et al., 1993), which encodes a 315 kD protein that is also localized in knobs (Pasloske et al., 1993). Clearly, more precise studies are needed to understand better the function of such proteins in infected cells.

Recently, methodologies for both transient (Wu et al., 1995) and stable (Crabb and Cowman, 1996; Wu et al., 1996) transfection of P. falciparum were developed. These studies showed that plasmid constructs that possessed the selectable marker Toxoplasma gondii dihydrofolate reductase–thymidylate synthase (*TgDHFR–TS*), which had been mutated to confer resistance to the anti-folate drug pyrimethamine, could be maintained episomally in infected parasites. Following an extended period of in vitro culture, plasmids integrated into the P. falciparum genome, in general, by a process of homologous integration (Crabb and Cowman, 1996; Wu et al., 1996). This occurred despite the presence of only relatively short homologous sequences in the various

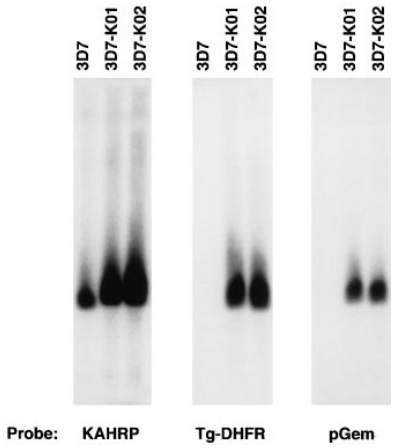

Figure 1. PFGE Showing Chromosomes from the Parental 3D7 and Transfected Parasite Clones 3D7-KO1 and 3D7-KO2

Following transfer to a nitrocellulose membrane, the identical filters were hybridized with *KAHRP*, *TgDHFR–TS*, and pGem.

plasmid constructs. It was clear that targeted gene disruption experiments were now a distinct possibility.

In this paper, we describe the targeted disruption of the gene encoding KAHRP by transfection of the KAHRP-positive (K^+) P. falciparum parasite line and show that this protein is essential for knob formation. The distribution of PfEMP1 is different in K^- transgenic lines, suggesting that KAHRP is involved in the localization of PfEMP1. Analysis of the adherence properties of the parental and transgenic parasite lines shows that a biological function of knobs in P. falciparum is to enable parasitized cells to cytoadhere to microvascular endothelium under physiologically relevent flow conditions.

Results

Disruption of the *KAHRP* Gene

To disrupt the *KAHRP* gene in P. falciparum, a plasmid vector (pTgD-TS.CAM5/3.KP), which comprises a selectable gene flanked by two halves of the second exon of the *KAHRP* gene, was constructed (see Figure 2C) (Crabb and Cowman, 1996). The selectable gene cassette comprised the *TgDHFR–TS* gene, which was modified to confer resistance to pyrimethamine and flanked by the P. falciparum calmodulin promoter and 3′-untranslated regions. The construct was transfected into the K^+ cloned P. falciparum line, 3D7, which is known to be sensitive to pyrimethamine. In order to select for parasites possessing integrated plasmids, the concentration of pyrimethamine was increased, and the transfectants cultured for a further 4 weeks, at which point they were cloned. Chromosomes from the parent line, 3D7, and two randomly selected clones, 3D7-KO1 and 3D7-KO2, were separated by pulsed-field gel electrophoresis (PFGE), transferred to a nylon filter, and probed with the *KAHRP* gene (Figure 1). The *KAHRP* gene is located on chromosome 2 (Corcoran et al., 1986), and the probe hybridized to this chromosome in 3D7 as well as 3D7-KO1 and 3D7-KO2. An identical filter was probed with the *TgDHFR–TS* gene, and hybridization to the 3D7 parent was not observed, whereas hybridization to chromosome 2 was obtained for both 3D7-KO1 and 3D7-KO2. Therefore, it was apparent that the selectable marker had integrated into chromosome 2 of both cloned lines. An identical pattern of hybridization, as obtained for the *TgDHFR–TS* probe, was observed with the plasmid probe pGem, which showed that the plasmid backbone also had integrated into chromosome 2. This indicated that integration did not involve a double-crossover event into *KAHRP*, a process that would have deleted the plasmid backbone.

In order to test if the transfected plasmid had integrated into the *KAHRP* gene on chromosome 2, genomic DNA from 3D7 and 3D7-KO1 was digested with BamHI and EcoRI prior to Southern blotting. Filters were probed with the *KAHRP* exon 2/half1 DNA fragment (Figure 2D). In 3D7, a 7.4 kb BamHI fragment was observed, whereas in 3D7-KO1 the probe hybridized to two BamHI fragments of 7.8 and 1.9 kb (Figure 2A). Hybridization of the same probe to an EcoRI digest revealed a 17 kb fragment in 3D7, whereas 3D7-KO1 showed a fragment of 22 kb and a second fragment of 3.9 kb. These results are consistent with homologous integration of a single copy of the transfection plasmid into the *KAHRP* exon 2/half1 region by a single-crossover event (Figure 2D). To confirm this, the restriction enzyme digests of genomic DNA from 3D7 and 3D7-KO1 were probed separately with the *TgDHFR–TS* and pGem DNA fragments (Figures 2A and 2D). These probes did not hybridize, as expected, to the 3D7 parent line. However, hybridization patterns obtained with 3D7-KO1 (Figure 2A) were consistent, with a single-crossover event occurring in the *KAHRP* exon 2/half1 region (Figure 2D). Identical results were obtained with genomic DNA prepared from the transfected cloned line 3D7-KO2, as well as the uncloned parental transfectants, 3D7-tran1, and a second independent transfection experiment, 3D7-tran2 (data not shown). These results showed that the pTgD-TS.CAM5/3.KP plasmid had integrated into the *KAHRP* coding region in a manner that would disrupt the expression of KAHRP.

KAHRP Is Not Expressed in the P. falciparum Transfectants

Proteins from synchronized trophozoite-stage parasites of 3D7, 3D7-KO1, 3D7-KO2, 3D7-tran1, and 3D7-tran2 were examined by immunoblot analysis. Membranes were probed with a rabbit anti-KAHRP antiserum that was raised to a hexahistidine fusion protein comprising a region of the KAHRP protein. The antisera reacted with a protein of ~110 kDa in the parent line 3D7 but did not react with a protein of this size in 3D7-KO1, 3D7-KO2, 3D7-tran1, and 3D7-tran2 (Figure 3). An identical filter was probed with an anti-hsp70 antiserum, and a protein corresponding to hsp70 (70 kDa) (Bianco et al., 1986) was detected in approximately equal amounts in each cloned line, showing that an equal amount of protein was loaded in each track (Figure 3). Therefore, integration of the plasmid pTgD-TS.CAM5/3.KP into the *KAHRP* gene of 3D7-KO1, 3D7-KO2, 3D7-tran1, and 3D7-tran2 has resulted in the loss of expression of this protein.

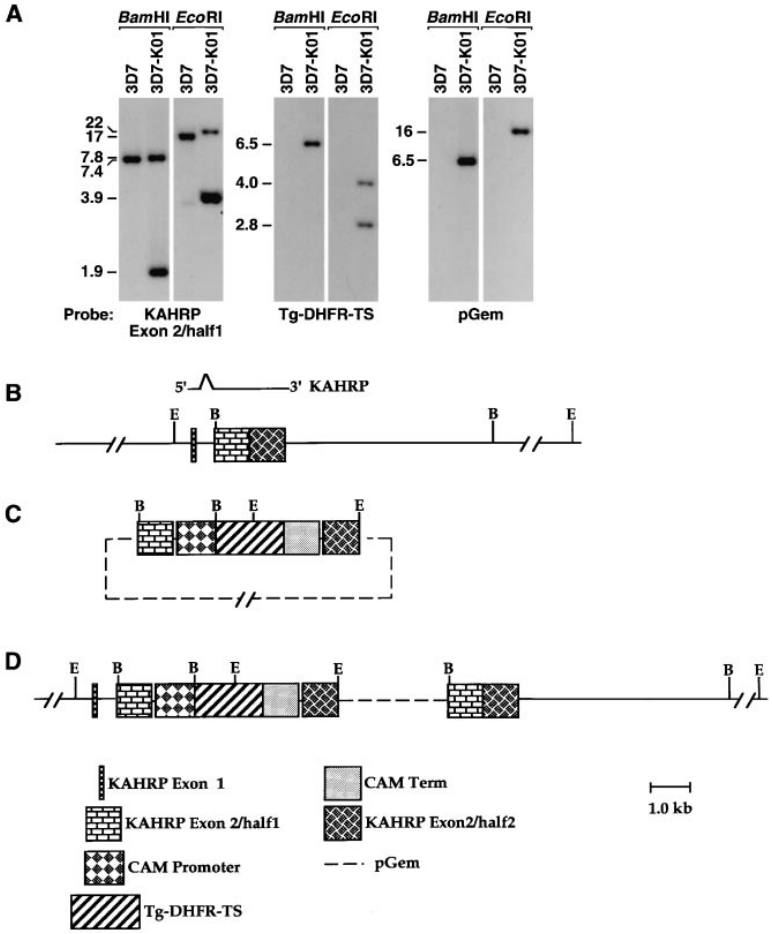

Figure 2. Analyses of Genomic DNA Showing Homologous Integration into the *KAHRP* Gene of the 3D7 P. falciparum Cloned Line

(A) Genomic DNA from 3D7, 3D7-KO1, and 3D7-KO2 was digested with BamHI and EcoRI, separated on 0.7% agarose gels, and blotted to nylon membranes. Membranes were hybridized with *KAHRP* exon2/half1, *TgDHFR–TS*, and pGem as shown at the bottom of (A).

(B) Schematic representation of the structure of the *KAHRP* gene and transcript. The spliced mRNA of the *KAHRP* gene is shown above the gene.

(C) Schematic representation of the plasmid vector pTgD-TS.CAM5/3.KP used for stable transformation of P. falciparum.

(D) The proposed model of integration of pTgD-TS.CAM5/3.KP into the *KAHRP* gene.

The restriction sites for (B), (C), and (D) are EcoRI ("E") and BamHI ("B"). The code for each of the schematic diagrams and the scale in (B), (C), and (D) is shown at the bottom of Panel (D).

KAHRP Expression Is Necessary for the Formation of Knob Structures

KAHRP is one of several proteins associated with knobs on mature parasites (Kilejian, 1979). To determine if this protein is essential to the formation of this structure, mature trophozoites from 3D7, 3D7-KO1, and 3D7-KO2 were analyzed by scanning electron microscopy and transmission electron microscopy. Scanning electron micrographs of 3D7 (Figure 4A) showed a typical knobbed surface present on the infected erythrocyte plasma membrane; however, 3D7-KO1 and 3D7-KO2 show a smooth erythrocyte membrane surface (Figure 4D). Transmission electron microscopy of 3D7 showed the presence of numerous electron-dense structures that have been previously identified as knobs (Figures 4B and 4C) (Kilejian, 1979). These structures were absent in 3D7-KO1 and 3D7-KO2 (Figures 4E and 4F). More than 100 individual parasites were examined by transmission electron microscopy in each parasite line, and 70% of 3D7 trophozoites showed clearly evident knob structures, whereas these were not detected in any of the trophozoite-stage parasites examined from 3D7-KO1 and 3D7-KO2. Therefore, expression of KAHRP is essential for formation of knobs in P. falciparum.

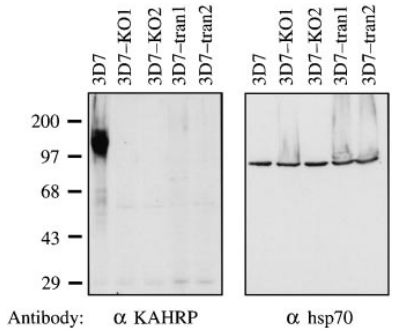

Figure 3. The KAHRP Protein Is Not Expressed in 3D7-KO1, 3D7-KO2, 3D7-tran1, and 3D7-tran2

Proteins from synchronized trophozoites were separated by SDS–PAGE and blotted to nylon filter. Identical filters were probed with either antibodies to the Hexahis-KAHRP fusion protein (left panel) or antibodies to the P. falciparum hsp70 protein (Bianco et al., 1986).

Localization of PfEMP1 in K⁻ Transfectants

To examine the distribution of PfEMP1 in the K⁻ transfectants, 3D7-KO1, 3D7-KO2, 3D7-tran1, and 3D7-tran2 were compared to the 3D7 parental clone by immunofluorescence using an antisera raised to the acidic terminal section (ATS) (Baruch et al., 1995; Su et al., 1995) from a *var* gene in the 3D7 P. falciparum cloned line. Affinity-purified anti-ATS antibodies were analyzed for specificity by immunoblots to GST protein and the GST–ATS fusion protein. These antibodies did not react with the

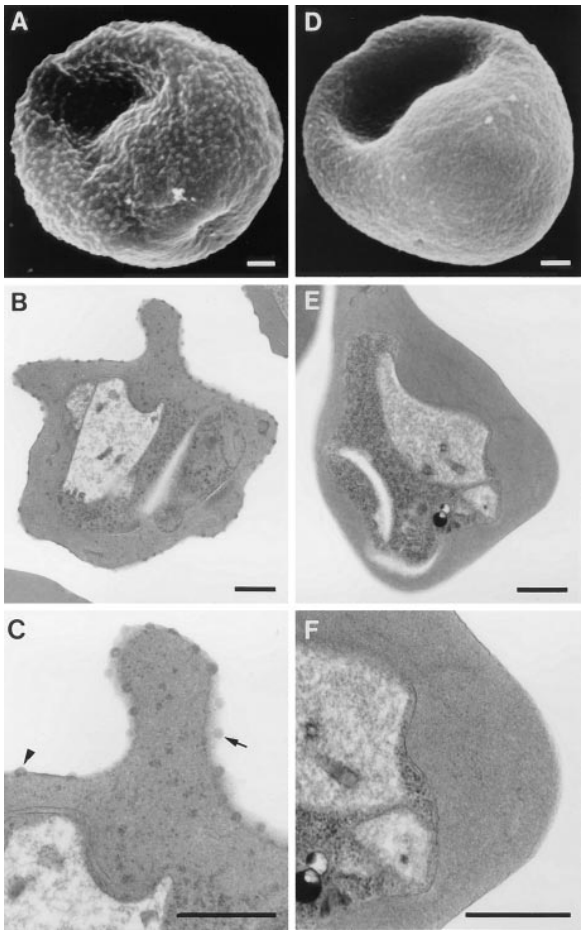

Figure 4. P. falciparum Trophozoite-Infected Erythrocytes Displaying the Knob and Knobless Morphologies

(A) Percoll-purified trophozoites of 3D7-infected erythrocytes were visualized by scanning electron microscopy.

(B and C) Trophozoite-infected erythrocytes of clone 3D7 possess knobs (sectioned tangentially [arrow] and transversely [arrowhead] in [C]).

(D) Percoll-purified trophozoite-infected erythrocytes of 3D7-KO1 visualized by scanning electron microscopy.

(E and F) Trophozoite-infected erythrocytes infected with 3D7-KO1. A total of 100 cells infected with clone 3D7-KO1 and 100 cells infected with clone 3D7-KO2 were observed, and no cells contained knobs. Scale bar = 0.5 μm.

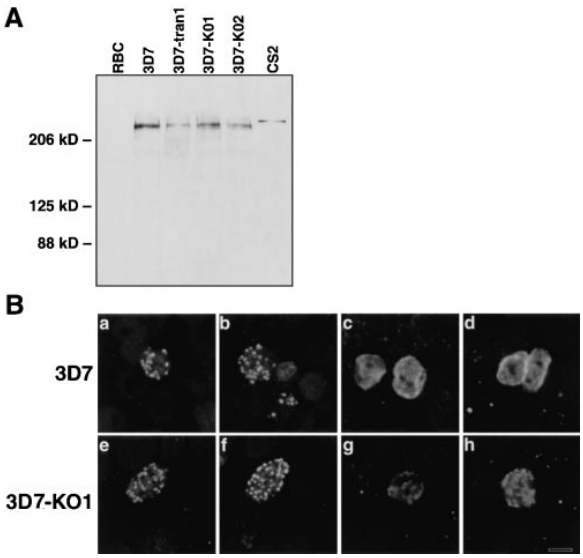

Figure 5. Characterization of PfEMP1 in *KAHRP* Knockouts

(A) Immunoblotting of different lines of P. falciparum using the affinity-purified anti-ATS antibodies to detect the PfEMP1 proteins. Proteins from SDS extracts of 2×10^5 trophozoites were seperated by SDS–PAGE, transferred to polyvinylidene difluoride membrane, and incubated with affinity-purified rabbit anti-ATS antibodies for 1 hr at room temperature. Bound antibodies were visualized using the ECL Western blot method.

(B) Localization of PfEMP1 in 3D7 and 3D7-KO1 by immunofluorescence and confocal microscopy using anti-ATS antibodies. Affinity-purified antibodies to the ATS domain of a *var* gene from 3D7 were reacted with acetone/methanol-fixed smears of each cloned line. Following incubation with FITC-labeled goat anti-rabbit antibody, smears were visualized by laser-confocal microscopy. The P. falciparum cloned lines shown are as follows: late rings with no pigmented cells, 3D7 (a and b), 3D7-KO1 (e and f); mature trophozoites with all cells pigmented, 3D7 (c and d), 3D7-KO1 (g and h). The images shown were chosen randomly and are representative of the vast majority of fluorescent cells observed in each sample. All images were captured under identical conditions and intensity. The size bar in (h) represents 5 μM and is the same for all panels.

GST protein but did react strongly to the GST–ATS fusion protein (data not shown). Also, preincubation of the antibodies with the GST–ATS fusion protein removed reactivity to the GST–ATS protein (data not shown). These results showed that the affinity-purified antibodies are specific to the ATS portion of the fusion protein.

To show that the affinity-purified anti-ATS antisera reacted with a protein that had the expected properties of PfEMP1, we extracted Triton X-100-insoluble SDS-soluble proteins from 3D7, 3D7-KO1, 3D7-KO2, 3D7-tran1, and CS2 parasite lines. CS2, an E8B-derived line selected for adherence to chondroitin sulfate, was included as an example of a different parasite line. The proteins were separated by SDS–PAGE, and immunoblots probed with the affinity-purified anti-ATS antibodies. A large molecular mass protein of over 200 kDa was detected in extracts from parasitized RBC but not in uninfected RBC (Figure 5A). In the 3D7 parent and each of the transfected lines, the antibodies detected a major protein(s) of the same molecular mass. In contrast, the molecular mass of the protein detected in CS2 (Figure 5A) and in other parasite lines (data not shown) varied significantly. A single protein band was also detected in B8, a parasite line that has deleted a large portion of chromosome 2 including the gene encoding PfEMP3 (Biggs et al., 1989), suggesting that the antisera is not cross-reacting with this protein molecule (data not shown). Taken together, these data indicate that the anti-ATS antibodies bind PfEMP1 and that 3D7, 3D7-KO1, 3D7-KO2, and 3D7-tran1 express a PfEMP1 molecule(s) of the same size.

To determine if the pattern of expression of the PfEMP1 protein had altered between parental and *KAHRP*$^-$ knockout lines, the parasites were synchronized, and smears taken every 8 hr throughout the asexual life cycle of the parasite. No fluorescence was detected when either rabbit prebleed antibodies, rabbit anti-GST antibodies, or the FITC-goat anti-rabbit second antibody alone were used (data not shown). When

Table 1. Binding of Infected Erythrocytes to Purified Ligands

Cloned Line	ICAM-1	CSA-PE	CD36
3D7	2.8 ± 1.5	31.5 ± 8.7	1004 ± 162.8
3D7-KO1	0.3 ± 0.28	2.1 ± 1.1	1246 ± 111.4
3D7-KO2	3.1 ± 1.0	4.4 ± 2.1	732.7 ± 22.7

Results are expressed as parasites bound per mm^2 and show mean ± SEM for triplicate experiments.

probed with the anti-ATS antibody, fluorescence was not observed in smears of early ring-stage parasites (data not shown) but was clearly evident in late rings, where a punctate pattern of expression was observed in 3D7 and 3D7-KO1 (Figures 5Ba, 5Bb, 5Be, and 5Bf), as well as 3D7-KO2, 3D7-tran1, and 3D7-tran2 (data not shown). The punctate spots of fluorescence appeared to be located within the erythrocyte cytoplasm of the P. falciparum-infected cell, and some cells showed the large spots apparently aligned directly under the erythrocyte membrane. As the synchronized parasites developed, 3D7 showed a difference in the pattern of expression of PfEMP1 compared to the *KAHRP*$^-$ transfectants. 3D7 parental cloned line gave a pattern suggestive of strong surface fluorescence with no punctate pattern evident (Figures 5Bc and 5Bd); however, the 3D7-KO1 (Figures 5Bg and 5Bh), 3D7-KO2, 3D7-tran1, and 3D7-tran2 still had a punctate pattern. There was clearly fluorescence suggestive of surface labeling, but this was not as intense or as uniform as that seen in 3D7. An identical pattern of fluorescence was observed when the smears were probed with an antibody made to the DBL region of a *var* gene (data not shown). The differential localization of PfEMP1 in 3D7 compared to 3D7-KO1, 3D7-KO2, 3D7-tran1, and 3D7-tran2 showed that KAHRP (and/or knob) expression is important in the localization of PfEMP1 and appears to be involved in trafficking PfEMP1 to the erythrocyte surface and/or in correctly distributing PfEMP1 once on the surface.

Knobs Are Important for Cytoadherence under Physiological Flow Conditions

To assess the role of knobs in cytoadhesion, we quantified adhesion of parasitized cells to known endothelial cell-expressed receptors using both static and flow-based assays. In static assays, all parasitized cells adhered well to CD36 with no apparent differences in the level of adhesion between the 3D7 parent and either of the transfected clones 3D7-KO1 and 3D7-KO2 (Table 1). In contrast, there was no significant adhesion of any parasite line to intercellular adhesion molecule-1 (ICAM-1) or chondroitin sulfate A (CSA) when tested in the same assay. Also, the uncloned transfected lines 3D7-tran1 and the second independent line 3D7-tran2 showed equivalent levels of binding to CD36 as the 3D7-KO1 and 3D7-KO2 cloned lines in static assays (data not shown).

Previously, it has been shown that PfEMP1-mediated adherence is highly sensitive to inhibition with incubation of parasitized cells to trypsin. In order to strengthen the evidence that binding to CD36 is mediated by PfEMP1, we incubated 3D7 and 3D7-KO1 with varying concentrations of trypsin before testing for adherence to purified CD36. Adhesion to CD36 was significantly decreased after incubation with 1 μg/ml of trypsin for both 3D7 and 3D7-KO1 and completely ablated if the concentration of trypsin was raised to 10 μg/ml (Table 2). Coincubation of the cells with trypsin and soybean trypsin inhibitor did not affect adhesion to CD36, showing that the disappearance of binding was due to digestion of a protein molecule on the infected erythrocyte membrane. The exquisite protease sensitivity of the CD36-mediated adhesion of 3D7 and 3D7-KO1 supports the contention that this interaction is mediated via PfEMP1 expressed on the red cell membrane surface, and this datum is consistent with the pattern of immunofluorescence seen with the anti-ATS antisera.

Table 2. Adherence of 3D7 and 3D7-KO1 to CD36 Is Trypsin Sensitive

Trypsin Concentration (μg/ml)	Binding (% of control)	
	3D7	3D7-KO1
Control	100	100
1.0	26.5	11
10	2.9	1
100	0	0
10 + STI[a]	115	169

Results are from one experiment. Assays were performed in quadruplicate and are expressed as mean adherence to CD36 as a percentage of control.
[a]Trypsin (10 μg/ml) and soybean trypsin inhibitor (100 μg/ml) were added simultaneously to controls.

Although adhesion of the 3D7 parental line compared to the *KAHRP*$^-$ knockout lines was similar under static conditions, a more physiologically relevant measure is under conditions that mimic wall shear stresses found in the microvascular compartment where P. falciparum is known to sequester. Therefore, adhesion was quantified under flow at different wall shear stresses. Under these conditions, dramatic differences were observed between the adhesive capacity of the K^+ and K^- parasites (Figure 6). When flowed through the flow chamber, all parasite lines tested were able to adhere to the platelet monolayer at wall shear stresses in the range 0.05–0.3 Pa, although the absolute level of adhesion was highly shear dependent; that is, the number of parasitized cells that adhered was highest at 0.05 Pa but decreased monotonically with increasing stress. Importantly, the 3D7 parental line adhered at levels four to five times higher when compared to 3D7-KO1 or 3D7-KO2 lines under identical flow conditions (Figures 6A and 6B). Similar results were obtained with the uncloned independent transfectants 3D7-tran1 and 3D7-tran2 (Figure 6B). For all five parasite lines, parasitized cells formed stationary, rather than rolling, interactions (Cooke et al., 1994).

In order to make a quantitative estimation of the strength of the adhesive interaction, we measured the ability of adherent parasitized cells to withstand detachment by increasing levels of wall shear stress (Figure 6C). On average, the wall shear stress to detach 50% of adherent parasitized cells for the 3D7-KO1, 3D7-KO2, 3D7-tran1, and 3D7-tran2 transfected lines was 0.33 Pa compared to 0.95 Pa for the 3D7 parent line. Taken together, these results show that the K^- transfected

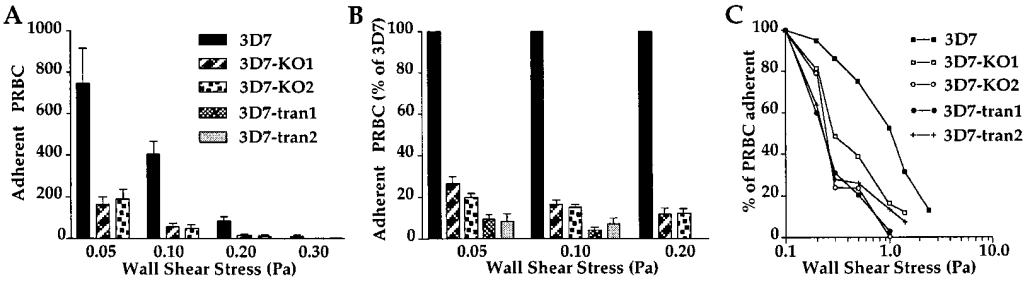

Figure 6. Adhesion of 3D7, 3D7-KO1, 3D7-KO2, 3D7-tran1, and 3D7-tran2, to Platelet-Expressed CD36 under Flow Conditions

(A) Variation in the number of flowing parasitized cells that adhered to a platelet monolayer in the flow chamber at various wall shear stresses over the range 0.05–0.30 Pa. At each stress, adherent parasite-infected red cells were counted in a number of precalibrated microscopic fields (each of area 0.17 mm^2), then expressed as adherent parasitized cells/$mm^2/10^7$ parasitized cells perfused to normalize for differences in parasitemia between experiments and allow for differences in flow rate at the different wall shear stresses. Data represent the mean ± SEM from three to five separate experiments using platelet-coated flow chambers from a single batch.

(B) The same data from (A) and equivalent experiments for 3D7-tran1 and 3D7-tran2 at wall shear stresses of 0.05 and 0.1 Pa, but adhesion of the K^- lines at each level of wall shear stress is expressed relative to the number of K^+ parasitized cells that adhered (normalized to 100%).

(C) The effect of increasing levels of wall shear stress on the number of parasitized cells that remained adhered to the platelet monolayer in the flow chamber. Parasitized cells were first allowed to adhere at 0.1 Pa, then exposed to stepwise increases in the level of wall shear stress. Data are shown from one typical experiment and represent the number of parasitized cells that remained adherent at each level of wall shear stress (expressed relative to the number initially adherent at 0.1 Pa).

lines adhere poorly, with low bond strength, to CD36 at wall shear stresses that reflect the levels proposed to exist in the microcirculation in vivo (Chien, 1972; Turitto, 1982).

3D7 and *KAHRP* Knockout Parasite Lines Express the Same *var* Genes

To address the possibility that expression of a different PfEMP1 protein in the *KAHRP*$^-$ parasite transfectants was responsible for the different adherence properties under flow conditions, we characterized the *var* gene transcripts in each of the 3D7 lines. RNA from each parasite line was used for RT–PCR using three different sets of oligonucleotide primers (Figure 7A) to exclude the possibility of differential priming. Also, the oligonucleotides extended over the intron of the *var* genes to ensure that expressed transcripts were being analyzed. The SVL region of *var* genes is very diverse between the genes that have been analyzed. However, there are conserved motifs that enable degenerate oligonucleotides to be used in RT–PCR experiments.

Sequence analysis of the *var* gene transcripts in 3D7, 3D7-KO1, 3D7-KO2, 3D7-tran1, and 3D7-tran2 showed that each of these parasite lines expressed one predominant *var* gene, termed "type a" (Figure 7B). A second *var* gene (type b) was detected in 3D7, 3D7-KO2, and 3D7-tran1, but this appeared to be present at lower levels than the "type a" gene. Use of the same oligonucleotide primers similarly to analyze cloned lines derived from 3D7 that had been selected for binding to chondroitin sulfate and ICAM-1 respectively, showed that these lines express different *var* genes to those seen in the parental 3D7 and the *KAHRP* knockout lines (M. E. W. and A. F. C., unpublished data). This suggests that the oligonucleotides used in the PCR analysis gave a true representation of the *var* genes expressed by the different parasite lines. The transcript analysis of the *var* gene is consistent with the detection of a major protein band of the same size in 3D7 and the different *KAHRP*$^-$ knockout clones. This datum is strongly indicative of the parental and *KAHRP*$^-$ knockout lines expressing the same predominant *var* gene and attributes the differences in adhesion under flow conditions to the absence of KAHRP and knobs and not to a *var* gene switch. The detection of two *var* gene transcripts in some of the cloned lines suggests either that a single parasite can express two *var* genes or that there is a favoured switch event to the minor *var* gene detected in some of the 3D7 parasite lines.

Discussion

Upon infection with a malaria parasite, an interesting set of changes occurs to the human erythrocyte. In essence, it is converted into a more typical, although still

A

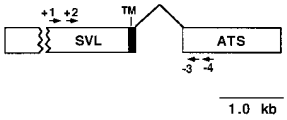

B

oligonucleotide pair	*var* gene sequence									
	3D7		3D7-KO1		3D7-KO2		3D7-tran1		3D7-tran2	
	a	b	a	b	a	b	a	b	a	b
+2,-4	3	0	1	0	0	0	1	0	3	0
+1,-4	0	0	2	0	2	1	2	1	1	0
+1,-3	2	1	2	0	3	2	1	1	1	0
total	5	1	5	0	5	3	4	2	5	0

Figure 7. Sequencing of RT–PCR-Derived cDNA from 3D7, 3D7-KO1, 3D7-KO2, 3D7-tran1, and 3D7-tran2 Shows That Parental and *KAHRP*$^-$ Knockouts Express One Predominant *var* Gene

(A) Structure of the 3′ end of a P. falciparum *var* gene and the position of the different degenerate oligonucleotides used in RT–PCR experiments to obtain cDNA from each parasite line for sequencing. SVL, segment of variable length; ATS, acid terminal segment; TM, transmembrane segment. Only the relevant section of the *var* gene is shown.

(B) Sequence analysis of the cDNA clones from each parasite line. The numbers represents the number of clones of sequence type "a" or "b" identified in each parasite line.

relatively simple, eukaryotic cell by the appearance of new structures in the red cell cytoplasm and new proteins at the red cell membrane (Deitsch and Wellems, 1996). At least eight parasite proteins that bind to the red cell cytoskeleton have been identified, but for most of these no functional role has been ascribed. The development of gene-targeting technology for P. falciparum provides a means to understand the role of these proteins in the structural and functional changes induced in erythrocytes by infection. In this work, we have used gene targeting to disrupt the gene encoding KAHRP.

It was of some note that genomic analysis of eight independent clones and of the uncloned transfectant revealed that each had integrated by the same single-crossover event, despite the plasmid construct being designed to integrate by a double-crossover event and possessing other sites (noncoding sequences) for homologous recombination. One possibility for this was that the number of integration events that occured in the selected parasite population may have been very few. We consider this unlikely, since, following the selection procedure, virtually all parasites in the uncloned population possessed integrated rather than episomal forms. This was in contrast to transfections performed previously that showed homologous integration into noncoding sequences (Crabb and Cowman, 1996; B. S. C. et al., unpublished data). In these instances, following the selection period, the majority of the transfected parasites still possessed episomal forms of the plasmid. Also, a second independent transfection of the *KAHRP* knockout plasmid into 3D7 yielded results identical to those obtained in the first transfection. It is therefore likely that with this plasmid, at least, the single-crossover event observed occured relatively frequently and was strongly favoured over other integration events.

This study shows that expression of KAHRP is essential for the formation of knobs on P. falciprum-infected erythrocytes. While other proteins are present in knob structures, the presence of KAHRP is obligatory for their formation. The formation of knobs clearly requires the assembly of knob-associated proteins into some sort of macromolecular structure, the mechanisms of which remain to be elucidated. The role of PfEMP3, or other knob-associated proteins, in knob formation is presently unknown. Targeted gene distruption of these proteins would provide important parasite lines to address this question.

Our observation that the K^- transfected parasites were able to adhere to purified CD36 in static assays as efficiently as the parent indicates that a CD36-adherence receptor remains functional and is retained on the surface of parasitized erythrocytes, despite the absence of KAHRP and knobs. A number of molecules capable of binding CD36 have been described on the surface of the infected red cell, including PfEMP1 (Ockenhouse and Chulay, 1988; Baruch et al., 1996), sequestrin (Ockenhouse et al., 1991), and aggregated band 3 (Crandall et al., 1993). No studies are available to quantitate their respective contributions to the total binding ability of the infected erythrocyte; however, we consider it likely that the majority of CD36 adherence is due to PfEMP1. PfEMP1 is clearly identified as a trypsin-sensitive molecule (Leech et al., 1984), and we show here that CD36 adherence of both the K^+ parent and K^- transfected lines is highly sensitive to trypsin. From the point of view of assigning a function to KAHRP, it is of little consequence whether the observed adherence was due to PfEMP1 alone or a combination of two or three CD36-binding molecules. In the absence of KAHRP, infected cells adhere poorly when physiological shear stresses that simulate those found in the microvasculature are applied.

Adhesion to CD36 was tested using activated platelets to ensure the proper conformation of CD36 (Cooke and Nash, 1995). We noted that for any given shear stress, the K^- transfected clones adhered about 5-fold less efficiently than the K^+ parent line. Furthermore, for those parasitized cells that were able to adhere, K^- transfected clones were about 3-fold easier to detach. This strongly suggests that the biological role of knobs is to permit adhesion of flowing parasitized cells in the hemodynamic environment of the microcirculation and, once adhered, to strengthen the interaction so that parasitized erythrocytes can withstand detachment by the shear stresses found in the human vasculature.

There are several possible ways that knobs can strengthen the interaction with ligands on the surface of endothelial cells. PfEMP1 has been shown to be enriched at the surface of knob structures (Baruch et al., 1995), implying that the cytoplasmic tail of PfEMP1 interacts with some component of the knob. The most likely candidate protein for this interaction is KAHRP, which itself is then linked to spectrin in the red cell cytoskeleton (Kilejian et al., 1991). The physical consequence of such an interaction is that extensional forces applied to PfEMP1 would be distributed over the surface area of the knob and increase the effective force that could be applied to PfEMP1 without its physical removal from the membrane. In a knob$^-$ line, PfEMP1 would be more weakly tethered to the membrane and the membrane skeleton. The differences in the localization of PfEMP1, as shown by immunofluorescence microscopy, between the transfected and parent parasite lines suggest that the interactions of the cytoplasmic tail of the receptor have been altered. Finally, it remains possible that KAHRP may actually assist in the transport to and orientation of PfEMP1 in the membrane.

Several lines of evidence exclude the possibility that the differences in adherence to CD36 under flow conditions observed between the parental line and the transfected lines were due to a switch to a new PfEMP1 protein that still binds to CD36 but with reduced affinity. Sequence analysis of spliced transcripts showed that the 3D7 parent and *KAHRP* knockout lines each express the same predominant *var* gene. This includes the progeny from two independent transfections, both of which express a *var* gene that is identical in sequence around the 3′ splice site. These results are consistent with the fact that the size of the PfEMP1 protein identified in each of the 3D7 derived lines is the same. As it is clear that these lines express the same predominant PfEMP1 proteins on the surface of the red cell, the phenotypic differences seen in adherence are due solely to the absence of KAHRP and knobs.

The ability to disrupt genes in P. falciparum will make it possible to analyze more easily and definitively the

function of many of the antigen genes that have been identified. The KAHRP protein is essential for knob formation and is therefore a key molecule in the interaction of the parasitized red blood cell with host capillaries. There is evidence that KAHRP interacts with spectrin and actin (Kilejian et al., 1991), and construction of a *KAHRP*$^-$ transfectant will enable the insertion of mutant forms of the *KAHRP* gene into the *KAHRP*$^-$ knob$^-$ parasite line to perform a structure–function analysis of this protein. This will be an important step in understanding the complex interactions between KAHRP, the red cell cytoskeleton, and PfEMPI.

Experimental Procedures

Parasites and Transfection

Parasites were cultivated (Trager and Jensen, 1978) and synchronized by standard procedures. Parasites were transfected as described for transient expression (Wu et al., 1995) with 100 μg of plasmid DNA that had been purified using Plasmid Maxi columns (Qiagen, Chatsworth, CA). Following transfection, parasites were returned to 150 cm^2 petri dishes and cultured for 48 hr before selection with 0.1 μM pyrimethamine (Crabb and Cowman, 1996; Wu et al., 1996). Transfected parasites were detectable after 3 weeks of continuous culture. Parasites containing integrated forms of the plasmid construct were selected by raising the pyrimethamine concentration to 1.0 μM for 4 weeks, followed by single-cell cloning. Construction of the plasmid vector pTgD-TS.CAM5/3.KP was described previously (Crabb and Cowman, 1996).

3D7 was obtained from Prof. David Walliker, Edinburgh University. E8B, a clone of Itg2, was obtained by three rounds of selection on melanoma cells. CS2 was obtained from E8B by three rounds of selection for adherence to chondroitin sulfate, followed by cloning (J. C. R. et al., unpublished data).

Nucleic Acids and Pulsed-Field Gel Electrophoresis

Genomic DNA was extracted from trophozoites as described (Coppel et al., 1987). All of the experiments involving manipulation of recombinant DNA and the analysis of nucleic acids by Southern blot hybridization were carried out using standard procedures. Chromosomes of P. falciparum were separated by pulsed-field gel electrophoresis (PFGE) using a contour-clamped homogeneous electric-field apparatus (Chu et al., 1986) at 4.2 V/cm and a pulse time of 225 s for 72 hr.

Poly(A)$^+$ RNA was purified from each parasite line using the MicroFast RNA extraction kit (Invitrogen), and cDNA synthesized using Microfast cDNA synthesis kit (Invitrogen). The expressed *var* genes were determined using degenerate oligonucleotides to different regions of the SVL and ATS for PCR reactions. Oligonucleotides used were; 1, GGWATWMGWRAAGATGWWTGGAAATG; 2, AAAMGWTG GGTWGAATATTTTTTAGAAGA; 3, CCWGGWACATAWATATCATT WATRTC; and 4, GGTTCTAAWACWACTTCWATTAAWGTTTTATAT TTW (W = A/T). The DNA products were cloned into a plasmid vector, and independent clones were sequenced.

Antisera and Western Blot Assays

Proteins from synchronized trophozoites were boiled in Laemmli buffer and separated on a 10% acrylamide-bisacrylamide (200:1) gel at 200 V. Proteins were transferred to nylon filters and probed either with rabbit antibodies made to a hexahistidine-KAHRP fusion protein or rabbit antibodies to the P. falciparum hsp70 protein at dilutions of 1 in 2000 (Bianco et al., 1986).

For the detection of PfEMP1, SDS-soluble proteins were extracted from trophozoite stages of different parasite lines and seperated on SDS–PAGE, followed by immunoblotting, as previously reported (Baruch et al., 1995). The filters were probed with rabbit antibodies to the ATS region of the major *var* gene expressed in 3D7. The ATS region used was from a very conserved region consisting of amino acids 2860–2988 (GenBank accession number L40608) and was obtained from cDNA by RT–PCR followed by cloning into the pGex vector; the GST–ATS fusion protein was purified on glutathione columns. Antibodies were made by immunization of rabbits with Freund's complete followed by Freund's incomplete adjuvant. Serum was depleted of anti-GST reactivity by passing three seperate times over a column of CNBr–Sepharose with coupled GST protein. Antibodies specific to the ATS portion of the fusion protein were obtained by affinity purification on CNBr–Sepharose with the GST–ATS fusion protein coupled. The absence of GST reactivity and specificity for ATS were confirmed by immunoblotting to the fusion protein and purified GST, as well as testing the ability of a preincubation with purified GST–ATS fusion protein to remove reactivity to the same fusion protein.

Electron Microscopy

Trophozoites for scanning electron microscopy were obtained by Percoll step-gradient purification as previously described (Cowman et al., 1991), and cells prepared by fixation in osmium tetroxide (1%) followed by standard dehydration and observation with a JEOL JSM-840 scanning electron microscope. Cells were prepared for transmission electron microscopy by fixation in glutaraldehyde (1.25%), then osmium tetroxide (1%), stained en bloc in uranyl acetate (2%), and embedded in Spurr's resin. Sections were examined with a JEOL JEM-1200EX transmission electron microscope.

Quantitation of Adhesion

Static assays for adhesion of parasitized cells to CD36, ICAM-1, and CSA immobilized onto 36 mm petri dishes were measured as described previously (Rogerson et al., 1995). Trypsin sensitivity of P. falciparum cytoadherence to purified CD36 was measured by resuspending the cell pellets in RPMI–HEPES containing trypsin (Sigma Chemical Co., St. Louis) at a final concentration of 100, 10, or 1 mg/ml. Soybean trypsin inhibitor (100 mg/ml; Sigma) was added similtaneously with trypsin (10 mg/ml) to controls. The tubes were incubated at 37°C for 30 min, and trypsin inhibitor added to each at a concentration 10× that of the protease. Serum (10%) was added to each to a final volume of 2 ml, and cytoadherence assays performed and results expressed as the number of parasitized cells bound/mm^2.

Flow-based assays for adhesion of parasitized cells were visualized and quantified under well-defined and carefully controlled flow conditions using the platelet-coated microslide method described previously (Cooke and Nash, 1995). Inhibition studies using monoclonal antibodies have previously shown that adhesion of parasitized cells to formalin-fixed platelets in this system is mediated almost entirely (>90%) by CD36 (Cooke and Nash, 1995). In brief, flow chambers were prepared by coating the lower internal surface of rectangular glass microcapillary tubes with a confluent monolayer of formalin-fixed human blood platelets. The chambers were then placed on the stage of an inverted phase-contrast light microscope and connected at both ends into a system that allows careful control of fluid flow through the chamber. Wall shear stresses in the range typical for postcapillary venules in vivo (Chien, 1972; Turitto, 1982) were calculated as a function of the volumetric flow rate of fluid through the chamber, which was carefully controlled using a Harvard syringe pump. The number of parasitized cells that adhered at a variety of wall shear stresses and the ability of cells, once attached, to withstand detachment by increasing levels of stress were quantified by following two protocols recently described in detail (Cooke et al., 1996). In brief, to quantitate adhesion from flow, parasitized cells were suspended in HEPES-buffered RPMI1640 containing 1% human serum at approximately 1.5×10^7 parasitized cells/ml, then flowed through the chamber for 5–10 min at a desired wall shear stress between 0.05 and 0.3 Pa. This was followed immediately by cell-free medium at the same stress for 5 min to wash away nonadherent cells. While flow was maintained, the platelet monolayer was viewed by direct microscopy, and adherent parasitized cells were counted in a number of precalibrated microscope fields. To quantitate detachment by flow, parasitized cells were allowed to adhere to the platelet monolayer at 0.1 Pa and quantified as above. Flow through the chamber was then increased in a stepwise manner to expose adherent cells to increasing levels of stress, each of 5 min duration. The number of parasitized cells remaining adherent were counted at each level of stress.

Immunofluorescence

3D7, 3D7-KO1, 3D7-KO2, 3D7-tran1, and 3D7-tran2 were synchronized with sorbitol, and smears were taken at 8 hr intervals. These were fixed in 90% acetone and 10% methanol for 2 min at room temperature. At the same time, smears were stained with Giemsa to determine visually the stage of the life cycle. Fixed smears were incubated with affinity-purified anti-ATS antibodies for 60 min at room temperature, washed, and incubated with FITC-conjugated goat anti-rabbit IgG antibodies (Silenus, Melbourne, Australia). The slides were washed and mounted in an antiquenching agent and visualized using a laser confocal microscope. All slides and images were treated in an identical manner.

Acknowledgments

We thank Anne Thaus for excellent technical assistance and Andrew Elephanty for assistance with the confocal microscopy. We thank S. Rogerson for helpful comments on this manuscript. This work was supported by the National Health and Medical Research Council of Australia, the National Institutes of Health (Grant DK32094–10), and Clive and Vera Ramaciotti Foundations. A. F. C. is supported by an International Research Scholars award from the Howard Hughes Medical Institute.

Received January 21, 1997; revised February 7, 1997.

References

Aikawa, M. (1988). Human cerebral malaria. Am. J. Trop. Med. Hyg. *39*, 3–10.

Barnwell, J.W., Asch, A.S., Nachman, R.L., Yamaya, M., and Aikawa, M. (1989). A human 88-kD membrane glycoprotein (CD36) functions in vitro as a receptor for a cytoadherence ligand on *Plasmodium falciparum*-infected erythrocytes. J. Clin. Invest. *84*, 765–772.

Baruch, D.I., Pasloske, B.L., Singh, H.B., Bi, X., Ma, X.C., Feldman, M., Taraschi, T.F., and Howard, R.J. (1995). Cloning the P. falciparum gene encoding PfEMP1, a malarial variant antigen and adherence receptor on the surface of parasitized human erythrocytes. Cell *82*, 77–87.

Baruch, D., Gormley, J.A., Ma, C., Howard, R.J., and Pasloske, B.L. (1996). *Plasmodium falciparum* erythrocyte membrane protein 1 is a parasitized erythrocyte receptor for adherence to CD36, thrombospondin, and intercellular adhesion molecule 1. Proc. Natl. Acad. Sci. USA *93*, 3497–3502.

Berendt, A.R., Simmons, D.L., Tansey, J., Newbold, C.I., and Marsh, K. (1989). Intercellular adhesion molecule-1 is an endothelial cell adhesion molecule for *Plasmodium falciparum*. Nature *341*, 57–59.

Bianco, A.E., Favaloro, J.M., Burkot, T.R., Culvenor, J.G., Crewther, P.E., Brown, G.V., Anders, R.F., Coppel, R.L., and Kemp, D.J. (1986). A repetitive antigen of *Plasmodium falciparum* that is homologous to heat shock protein 70 of *Drosophila melanogaster*. Proc. Natl. Acad. Sci. USA *83*, 8713–8717.

Biggs, B.A., Culvenor, J.G., Ng, J.S., Kemp, D.J., and Brown, G.V. (1989). *Plasmodium falciparum*: cytoadherence of a knobless clone. Exp. Parasitol. *69*, 189–197.

Biggs, B.A., Goozé, L., Wycherley, K., Wilkinson, D., Boyd, A.W., Forsyth, K.P., Edelman, L., Brown, G.V., and Leech, J.H. (1990). Knob-independent cytoadherence of *Plasmodium falciparum* to the leukocyte differentiation antigen CD36. J. Exp. Med. *171*, 1883–1892.

Chien, S. (1972). Present state of blood rheology. In Hemodilution. Theoretical Basis and Clinical Application, K. Messmer and H. Schmid-Schonbein, eds. (Basel: Karger), pp. 1–45.

Chu, G., Vollrath, D., and Davis, R. (1986). Separation of large DNA molecules by contour clamped homogeneous electric fields. Science *234*, 1582–1585.

Cooke, B.M., and Nash, G.B. (1995). *Plasmodium falciparum*: characterization of adhesion of flowing parasitized red blood cells to platelets. Exp. Parasitol. *80*, 116–123.

Cooke, B.M., Berendt, A.R., Craig, A.G., MacGregor, J., Newbold, C.I., and Nash, G.B. (1994). Rolling and stationary cytoadhesion of red blood cells parasitized by *Plasmodium falciparum*: separate roles for ICAM-1, CD36 and thrombospondin. Br. J. Haematol. *87*, 162–170.

Cooke, B.M., Rogerson, S.J., Brown, G.V., and Coppel, R.L. (1996). Adhesion of malaria-infected red blood cells to chondroitin sulfate A under flow conditions. Blood *88*, 4040–4044.

Coppel, R.L., Bianco, A.E., Culvenor, J.G., Crewther, P.E., Brown, G.V., Anders, R.F., and Kemp, D.J. (1987). A cDNA clone expressing a rhoptry protein of *Plasmodium falciparum*. Mol. Biochem. Parasitol. *25*, 73–81.

Corcoran, L.M., Forsyth, K.P., Bianco, A.E., Brown, G.V., and Kemp, D.J. (1986). Chromosome size polymorphisms in Plasmodium falciparum can involve deletions and are frequent in natural parasite populations. Cell *44*, 87–95.

Cowman, A.F., Karcz, S., Galatis, D., and Culvenor, J.G. (1991). A P-glycoprotein homologue of *Plasmodium falciparum* is localized on the digestive vacuole. J. Cell Biol. *113*, 1033–1042.

Crabb, B.S., and Cowman, A.F. (1996). Characterization of promoters and stable transfection in Plasmodium falciparum by homologous and non-homologous recombination. Proc. Natl. Acad. Sci. USA *93*, 7289–7294.

Crandall, I., Collins, W.E., Gysin, J., and Sherman, I.W. (1993). Synthetic peptides based on motifs present in human band 3 protein inhibit cytoadherence/sequestration of the malaria parasite *Plasmodium falciparum*. Proc. Natl. Acad. Sci. USA *90*, 4703–4707.

Culvenor, J.G., Langford, C.J., Crewther, P.E., Saint, R.B., Coppel, R.L., Kemp, D.J., Anders, R.F., and Brown, G.V. (1987). *Plasmodium falciparum*: identification and localization of a knob protein antigen expressed by a cDNA clone. Exp. Parasitol. *63*, 58–67.

Deitsch, K.W., and Wellems, T.E. (1996). Membrane modifications in erythrocytes parasitized by *Plasmodium falciparum*. Mol. Biochem. Parasitol. *76*, 1–10.

Howard, R.J., Barnwell, J.W., Rock, E.P., Neequaye, J., Ofori Adjei, D., Maloy, W.L., Lyon, J.A., and Saul, A. (1988). Two approximately 300 kilodalton *Plasmodium falciparum* proteins at the surface membrane of infected erythrocytes. Mol. Biochem. Parasitol. *27*, 207–224.

Kilejian, A. (1979). Characterization of a protein correlated with the production of knob-like protrusions on membranes of erythrocytes infected with *Plasmodium falciparum*. Proc. Natl. Acad. Sci. USA *76*, 4650–4653.

Kilejian, A., and Jensen, J.B. (1977). A histidine-rich protein from *Plasmodium falciparum* and its interaction with membranes. Bull. W.H.O. *55*, 191–197.

Kilejian, A., Rashid, M.A., Aikawa, M., Aji, T., and Yang, Y.F. (1991). Selective association of a fragment of the knob protein with spectrin, actin and the red cell membrane. Mol. Biochem. Parasitol. *44*, 175–182.

Langreth, S.G., and Peterson, E. (1985). Pathogenicity, stability, and immunogenicity of a knobless clone of Plasmodium falciparum in Colombian owl monkeys. Infect. Immun. *47*, 760–766.

Lanzer, M., De Bruin, D., and Ravetch, J.V. (1993). Transcriptional differences in polymorphic and conserved domains of a complete cloned *P. falciparum* chromosome. Nature *361*, 654–657.

Leech, J.H., Barnwell, J.W., Miller, L.H., and Howard, R.J. (1984). Identification of a strain-specific malarial antigen exposed on the surface of *Plasmodium falciparum*-infected erythrocytes. J. Exp. Med. *159*, 1567–1575.

MacPherson, G.G., Warrell, M.J., White, N.J., Looareesuwan, S., and Warrell, D.A. (1985). Human cerebral malaria. A quantitative ultrastructural analysis of parasitized erythrocyte sequestration. Am. J. Pathol. *119*, 385–401.

Ockenhouse, C.F., and Chulay, J.D. (1988). *Plasmodium falciparum* sequestration: OKM5 antigen (CD36) mediates cytoadherence of parasitized erythrocytes to a myelomonocytic cell line. J. Infect. Dis. *157*, 584–588.

Ockenhouse, C.F., Klotz, F.W., Tandon, N.N., and Jamieson, G.A.

(1991). Sequestrin, a CD36 recognition protein on *Plasmodium falciparum* malaria-infected erythrocytes identified by anti-idiotype antibodies. Proc. Natl. Acad. Sci. USA *88*, 3175–3179.

Ockenhouse, C.F., Tegoshi, T., Maeno, Y., Benjamin, C., Ho, M., Kan, K.E., Thway, Y., Win, K., Aikawa, M., and Lobb, R.R. (1992). Human vascular endothelial cell adhesion receptors for *Plasmodium falciparum*-infected erythrocytes: roles for endothelial leukocyte adhesion molecule 1 and vascular cell adhesion molecule 1. J. Exp. Med. *176*, 1183–1189.

Pasloske, B.L., Baruch, D.I., Van Schravendijk, M.R., Handunnetti, S.M., Aikawa, M., Fujioka, H., Taraschi, T.F., Gormley, J.A., and Howard, R.J. (1993). Cloning and characterization of a *Plasmodium falciparum* gene encoding a novel high-molecular weight host membrane-associated protein, PfEMP3. Mol. Biochem. Parasitol. *59*, 59–72.

Pologe, L.G., and Ravetch, J.V. (1986). A chromosomal rearrangement in a *P. falciparum* histidine-rich protein gene is associated with the knobless phenotype. Nature *322*, 474–477.

Pologe, L.G., Pavlovec, A., Shio, H., and Ravetch, J.V. (1987). Primary structure and subcellular localization of the knob-associated histidine-rich protein of *Plasmodium falciparum*. Proc. Natl. Acad. Sci. USA *84*, 7139–7143.

Raventos, S.C., Kaul, D.K., Macaluso, F., and Nagel, R.L. (1985). Membrane knobs are required for the microcirculatory obstruction induced by *Plasmodium falciparum*-infected erythrocytes. Proc. Natl. Acad. Sci. USA *82*, 3829–3833.

Rogerson, S.J., Chaiyaroj, S.C., Ng, K., Reeder, J.C., and Brown, G.V. (1995). Chondroitin sulfate A is a cell surface receptor for *Plasmodium falciparum*-infected erythrocytes. J. Exp. Med. *182*, 15–20.

Smith, J.D., Chitnis, C.E., Craig, A.G., Roberts, D.J., Hudson-Taylor, D.E., Peterson, D.S., Pinches, R., Newbold, C.I., and Miller, L.H. (1995). Switches in expression of Plasmodium falciparum *var* genes correlate with changes in antigenic and cytoadherent phenotypes of infected erythrocytes. Cell *82*, 101–110.

Su, X.-z, Heatwole, V.M., Wertheimer, S.P., Guinet, F., Herrfeldt, J.A., Peterson, D.S., Ravetch, J.A., and Wellems, T.E. (1995). The large diverse gene family *var* encodes proteins involved in cytoadherence and antigenic variation of Plasmodium falciparum-infected erythrocytes. Cell *82*, 89–100.

Trager, W., and Jensen, J.B. (1978). Cultivation of malarial parasites. Nature *273*, 621–622.

Turitto, V.T. (1982). Blood viscosity, mass transport, and thrombogenesis. Prog. Hemost. Thromb. *6*, 139–177.

Udeinya, I.J., Schmidt, J.A., Aikawa, M., Miller, L.H., and Green, I. (1981). *Falciparum* malaria-infected erythrocytes specifically bind to cultured human endothelial cells. Science *213*, 555–557.

Udomsangpetch, R., Aikawa, M., Berzins, K., Wahlgren, M., and Perlmann, P. (1989). Cytoadherence of knobless *Plasmodium falciparum*-infected erythrocytes and its inhibition by a human monoclonal antibody. Nature *338*, 763–765.

Wahlgren, M., Fernandez, V., Scholander, C., and Carlson, J. (1994). Rosetting. Parasitol. Today *10*, 73–79.

Wu, Y., Sifri, C.D., Lei, H.-H., Su, X.-S., and Wellems, T.E. (1995). Transfection of *Plasmodium falciparum* within human red blood cells. Proc. Natl. Acad. Sci. USA *92*, 973–977.

Wu, Y., Kirkman, L.A., and Wellems, T.E. (1996). Transformation of *Plasmodium falciparum* malaria parasites by homologous integration of plasmids that confer resistance to pyrimethamine. Proc. Natl. Acad. Sci. USA *93*, 1130–1134.